Geographic boundary and shear wave velocity structure of the "Pacific anomaly" near the core–mantle boundary beneath western Pacific

Yumei He [a],*, Lianxing Wen [b], Tianyu Zheng [a]

[a] Seismological Laboratory (SKL-LE), Institute of Geology and Geophysics, Chinese Academy of Sciences, Beijing 100029, PR China
[b] Department of Geosciences, State University of New York at Stony Brook, Stony Brook, New York, USA

Abstract

We determine the geographical boundary and shear-velocity structure of a very-low velocity province at the base of the Earth's mantle beneath western Pacific (we term it the "Pacific anomaly") based on the waveform modeling and travel time analysis of ScSH–SH phases. Our seismic data are from the China National Digital Seismographic Network, the F-net in Japan, the Global Seismographic Network and several PASSCAL arrays. The observed ScS–SH differential travel-time residuals allow the northwestern geographic boundary of the anomaly to be clearly defined. The seismic data also suggest that the average shear-velocity reduction inside the anomaly reaches −5% in the lowermost 300 km of the mantle. Waveform modeling of the seismic data sampling the edge of the anomaly suggests that the northwestern boundary is best characterized by a shear-velocity model with a velocity jump of about 2% at about 100–145 km above the core–mantle boundary and a thin (30-km thick) basal layer with a shear wave velocity reduction of −13%. Stacked seismic data sampling the middle of the anomaly, however, show no evidence for any internal discontinuity with a velocity decrease greater than −2% in the middle of the anomaly. Overall, the seismic data sampling the base of the "Pacific anomaly" can be explained by a negative shear-velocity gradient from 0% to −1% (top) to −13% (bottom) in the lowermost 220 km of the mantle, similar to those of a very-low velocity province beneath the South Atlantic Ocean and the Indian Ocean. Such a strong negative shear-velocity gradient can be explained by partial melting of a compositional anomaly produced early in the Earth's history located within a bottom thermal boundary layer. Our travel time data also exhibit small-scale variations inside the anomaly, indicating existence of internal small-scale seismic heterogeneities inside the "Pacific anomaly".
© 2006 Elsevier B.V. All rights reserved.

Keywords: shear wave velocity structure; core–mantle boundary; Pacific anomaly; compositional anomaly; African anomaly; very-low velocity province

1. Introduction

Seismic results have consistently shown two prominent low-velocity anomalies in the lower mantle, with one beneath Africa and the other beneath the Pacific Ocean [1–4]. Here, we refer to them as the "African anomaly" and the "Pacific anomaly". The geographic boundary, structural features and velocity structure of the "African anomaly" have been extensively studied and the nature is clear [5–10]. The "African anomaly" has a very-low velocity province (VLVP) as its base near the

core–mantle boundary (CMB) and regionally extends about 1300 km into the lower mantle. The VLVP exhibits an "L-shaped" form changing from a north–south orientation beneath the South Atlantic Ocean to an east–west orientation beneath the Indian Ocean, occupying an area of about $1.8 \times 10^7 \, km^2$ at the CMB. Seismic data also suggest that the VLVP has rapidly varying thicknesses from 300 km to 0 km above the CMB, steeply dipping edges, and a linear gradient of shear-velocity reduction from −2% (top) to −9% to −12% (bottom) relative to the Preliminary Reference Earth Model (PREM) [11] [5–8]. Those structural and velocity features indicate that the VLVP is compositionally distinct. The magnitude of shear-velocity perturbations of the VLVP would also require unreasonable temperature elevations, if the VLVP is purely a thermal anomaly [5]. For a compositional anomaly, an anomaly produced by the core–mantle reaction or segregation of subducted oceanic crust would not likely explain the unique presence and the steeply dipping edges of the "African anomaly". Thus, the most

plausible explanation of the seismic velocity structures of the VLVP is partial melt driven by a compositional change, produced early in the Earth's history [5–8].

The geographic boundary, velocity structure and origin of the "Pacific anomaly" are, however, less well defined. The "Pacific anomaly" is both structurally and characteristically different enough from the "African anomaly" that it is still under debate whether it represents an erupting thermal "superplume" from the CMB or is a chemically distinct anomaly. The seismic structures at the bottom of the mantle beneath the Pacific Ocean exhibit a complex pattern, in both length scale and velocity variation. The western Pacific region is characterized by many ultra-low velocity zones with P-velocity reductions as large as −10% and length-scales from tens of kilometers to hundreds of kilometers [12–20]. The central Pacific exhibits a 0% to −3% negative velocity gradient in the bottom 300 km of the mantle [7,21,22]. The southern Pacific is shown to exhibit a sharp lateral boundary at the base of the mantle [23]. As the recent studies of the "African anomaly" demonstrated, mapping

Table 1
Events for travel time analysis

Origin time	Latitude (°N)	Longitude (°E)	Depth (km)	Origin time	Latitude (°N)	Longitude (°E)	Depth (km)
1994.06.02.18.17.36	−10.47	112.98	39	1999.10.02.21.08.41	40.22	142.96	33
1994.06.15.09.22.57	−10.41	113.54	33	1999.10.24.04.21.41	44.61	149.44	33
1994.07.21.18.36.31	42.34	132.87	471	1999.10.25.20.31.42	−38.70	175.80	159
1994.09.28.16.39.52	−5.77	110.33	643	1999.11.11.02.41.05	49.31	155.63	33
1994.10.09.07.55.38	43.90	147.91	23	1999.11.26.00.29.00	55.13	165.36	33
1994.10.12.06.43.41	13.74	124.52	33	2000.01.02.12.58.42	51.45	−175.56	33
1994.12.30.15.12.25	18.56	145.36	219	2000.01.28.14.21.07	43.05	146.84	61
1995.08.23.07.06.02	18.86	145.22	595	2000.04.21.04.35.17	51.42	−178.14	33
1996.06.09.01.12.16	17.44	145.46	149	2000.06.14.02.15.25	−25.52	178.05	605
1996.06.17.11.22.18	−7.14	122.59	587	2000.08.15.04.30.08	−31.51	179.73	358
1996.09.20.00.03.18	9.60	126.29	33	2000.12.18.01.19.21	−21.18	−179.12	628
1996.12.30.19.41.52	−3.99	128.10	33	2001.01.19.08.10.14	−11.66	166.38	50
1997.01.17.11.20.22	−8.90	123.54	111	2001.05.09.17.38.26	−10.32	161.23	68
1997.09.04.04.23.37	−26.57	178.34	625	2001.05.26.10.57.26	−20.29	−177.84	407
1998.03.29.19.48.16	−17.55	−179.09	537	2001.09.18.02.19.30	−7.49	127.74	131
1998.04.14.03.41.22	−23.82	−179.87	499	2001.10.08.18.14.27	52.73	160.2	56
1998.05.16.02.22.03	−22.23	−179.52	586	2001.11.05.23.07.11	−17.29	−179.25	564
1998.07.09.14.45.39	−30.49	−178.99	130	2001.12.02.13.01.53	39.40	141.09	124
1998.07.16.11.56.36	−11.04	166.16	110	2002.06.16.06.55.13	−17.87	−178.70	569
1998.07.19.15.58.38	−21.84	−175.79	72	2002.06.30.21.29.36	−22.20	179.25	620
1998.12.14.19.35.26	−15.06	167.31	140	2002.08.09.13.31.05	−16.31	−176.17	364
1998.12.27.00.38.26	−21.63	−176.38	144	2002.08.12.02.59.23	−19.52	168.95	114
1999.01.28.18.24.25	−4.58	153.66	101	2002.10.16.10.12.21	51.95	157.32	102
1999.04.09.12.16.01	−26.35	178.22	621	2003.05.19.10.43.22	−18.04	−178.67	564
1999.04.13.10.38.48	−21.42	−176.46	164	2003.05.26.19.23.27	2.35	128.86	31
1999.04.20.19.04.08	−31.83	−179.07	96	2003.05.26.23.13.29	6.76	123.71	566
1999.08.01.12.47.50	51.52	−176.27	33	2003.06.16.22.08.02	55.49	160.00	175
1999.08.06.00.32.41	49.93	156.26	58	2003.06.23.12.12.34	51.44	176.78	20
1999.09.10.08.45.15	45.81	150.24	33	2004.01.25.11.43.11	−16.83	−174.20	130
1999.09.18.21.28.33	51.21	157.56	60				

out the geographic extent, velocity structure and structural features of an anomaly is important to the understanding of the origin and dynamic consequences of the anomaly. In recent years, with the deployment of many broadband seismic networks in China, the F-net in Japan and many portable PASSCAL seismic arrays, it becomes possible to map out the geographic boundary and detailed seismic structures near the CMB beneath the western Pacific. A comparative study of the seismic structures beneath Africa and the western Pacific would further help us narrow down the best possible interpretations of the seismic structures and dynamic consequences of these two anomalies.

In this study, we determine geographic boundary and shear-velocity structure of the base of the "Pacific anomaly" in a region beneath the western Pacific (35°S– 30°N and 125–185°E) using ScSH–SH differential travel times, and constrain detailed structures in the northeastern edge of the anomaly based on waveform modeling. We discuss seismic data in Section 2, present detailed constraints on the shear-velocity structure and

geometry in Section 3, and discuss implications of the seismic results in Section 4.

2. Seismic data

We collect broadband tangential displacements recorded at a distance range between 55° and 85° for travel-time analysis. We select 59 earthquakes occurring from 1994 to 2004 with a total of 630 ScS–S travel-time residuals (see Table 1). Our seismic data provide dense sampling in a region near the CMB between 0–30°N and 130–165°E (Fig. 1). The use of ScS–SH differential travel times minimizes the effect of source mislocation and seismic heterogeneities in the upper mantle, as ScS and SH phases propagate along similar ray paths in the upper mantle (Fig. 2). Most of our ScS–S differential travel times are selected from the seismic data recorded at several permanent and temporary seismic arrays in east Asia, including the China National Digital Seismographic Network (CNDSN), the F-net in Japan, and several permanent stations in the Global Seismographic
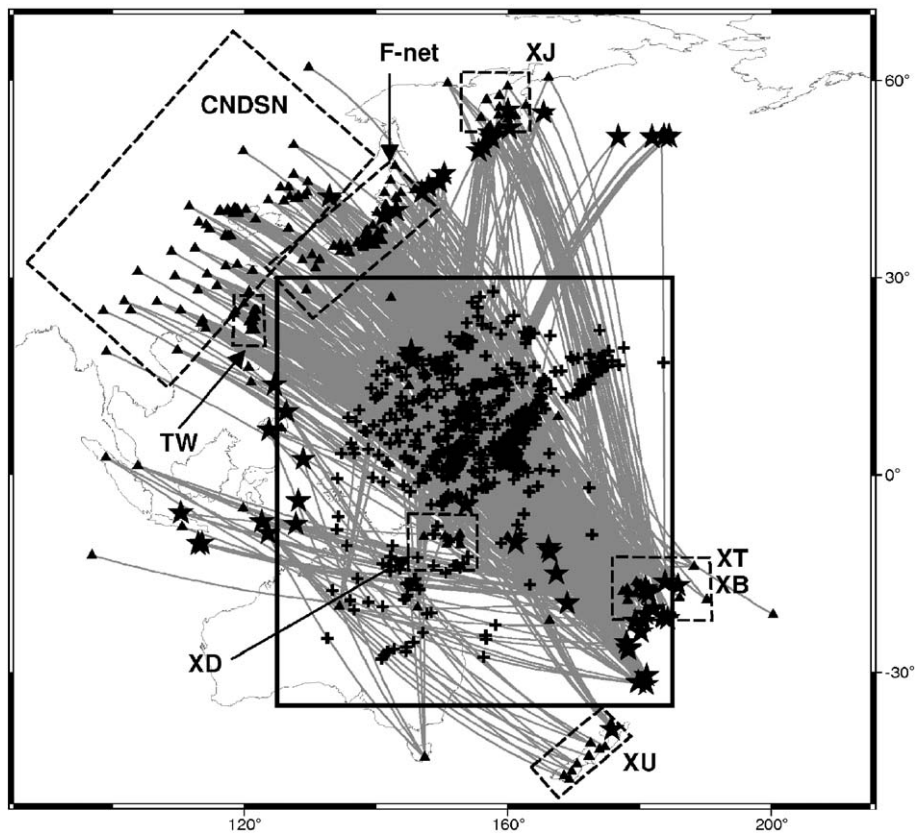

Fig. 1. The study region and ScS reflected points (crosses) at the CMB, along with earthquakes (stars), seismic stations (triangles), and great-circle paths (gray lines) of the seismic phases used in the study. The seismic networks are also labeled. The rectangle box indicates a region where detailed seismic results are presented in Fig. 3.
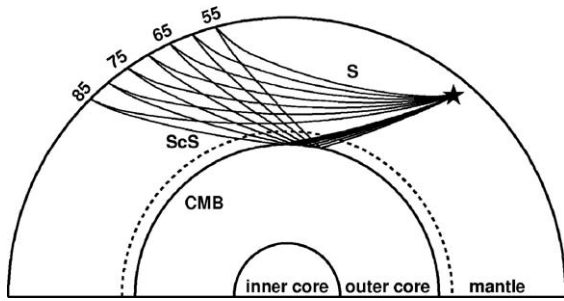
Fig. 2. S and ScS ray-paths based on PREM at epicentral distances from 55° to 85° for a source depth of 300 km.

Network (GSN), for earthquakes occurring in the Fiji subduction zone (Fig. 1). We also use the seismic data recorded in several PASSCAL arrays: the Southwest Pacific Seismic Experiment (XB), the Broadband Array in Taiwan for Seismology (TW), the Side Edge of Kamchatka Subduction Zone (XJ), the Woodlark-D_Entrecasteaux Rift, PNG (XD), the Micronesia Seismic Network (XT) and the New Zealand Seismic Experiment (XU), for earthquakes occurring in the sea of Okhotsk, the Japan Sea, the Java Sea, the Banda Sea, and the Philippine Islands. Data are selected based on their high signal-to-noise ratios. The broadband S and ScS signals are deconvolved with their instrumental responses and bandpass-filtered from 0.05 to 2 Hz.

We further use waveforms recorded in the Northern China Interior Structure Project (NCISP) and the Chinese Capital Seismic Network (CCSN) for two events occurring in the Tonga subduction zone to constrain the detailed seismic structures across the geographic boundary of the anomaly. The NCISP is a temporary broadband seismic array, deployed during 2000–2004 as part of the project to study the tectonic evolution and hydrocarbon accumulation in North China. It consists of 178 stations. Most of those stations were equipped with Reftek 72A-08 and 130-1 recorders and GMG-3ESP sensors. The CCSN is a network of broadband seismic stations deployed in the intersection of the Yanshan and Taihangshan in North China. The tangential waveforms are all bandpass-filtered from 0.08 to 2 Hz.

3. Geographic boundary and shear-velocity structure of the "Pacific anomaly" beneath western Pacific

3.1. Geographic boundary and overall shear-velocity structure based on ScS–S differential travel times

The ScS–S differential travel-time residuals provide good coverage in the lowermost mantle beneath the western Pacific (Fig. 3a). The ScS–S differential travel-time residuals vary from about −4 to 0 s in the northwest, west and southwest to 10 s in the east. The observed travel-time patterns indicate that these differential travel-time residuals are mainly caused by the travel-time variations of the ScS phases rather than those of the S phases. The travel-time residuals for the S phases show slightly negative correlation with the ScS–S travel-time residuals (Fig. 4a), while those for the ScS phases strongly correlate with the ScS–S differential travel-time residuals (Fig. 4b). Our primary interest is to use the ScS–S differential travel-time residuals to constrain the seismic structure in the lowermost 300 km of the mantle. The ScS–S differential travel-time residuals are insensitive to the seismic heterogeneities in the shallow mantle. However, at close distances, corrections are still required to account for the effects of seismic heterogeneities 300 km above the CMB, before one can attribute those differential travel-time residuals to the seismic structures in the lowermost 300 km of the mantle. We remove from the observed ScS–S differential travel-time residuals the contributions due to the seismic heterogeneities 300 km or more above the CMB based on predictions of several tomography models [1–4], and a recent model from Dr. Stephen Grand (personal communication). Corrections using various tomographic models yield slightly different, but similar results. We show an example of the difference of tomographic corrections, by presenting the relationships of the ScS–S differential travel-time residuals with S and ScS travel-time residuals before and after corrections using two tomographic models [Grand (personal communication), 2]. The correlations between the ScS travel-time residuals and the ScS–S differential travel-time residuals generally become stronger for the corrected data for both tomographic models (Fig. 4d and 4f), indicating that our corrections indeed improve minimizing the effects of seismic heterogeneities 300 km above the CMB on the ScS–S differential travel-time residuals. The corrections using other tomographic models yield correlations of ScS–S differential travel times and ScS travel times lying between these two cases. Such weak dependence on the tomographic models used in the corrections may be due to the similarities of the tomographic models in the region and more likely the fact that most of our observations are at large distances and those ScS–S differential travel-time residuals become insensitive to the seismic structures 300 km above the CMB. The latter is illustrated by the fact that the corrected ScS–S differential travel-time residuals exhibit similar patterns as the uncorrected ones (Fig. 4a
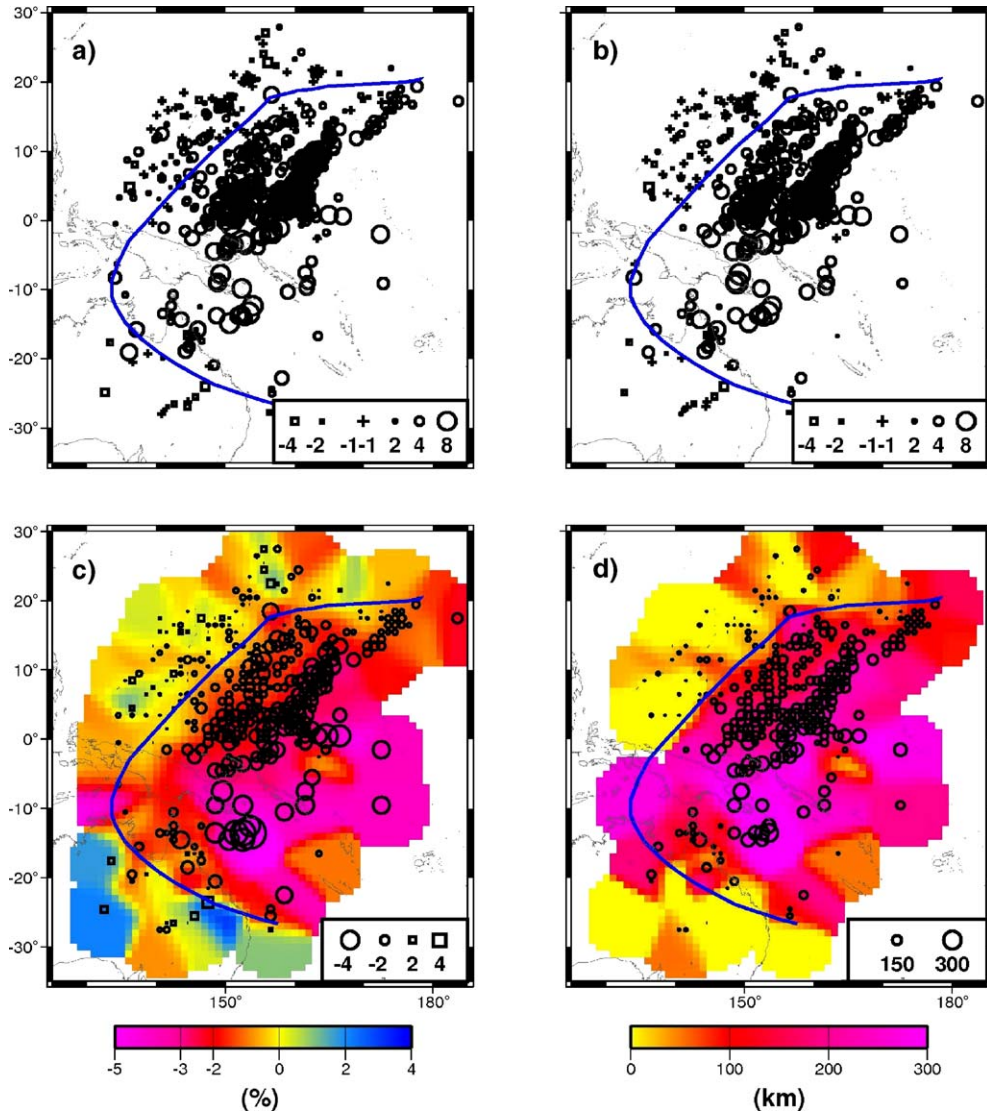
Fig. 3. (a) Observed ScS–S differential time residuals plotted at the ScS reflected points at the CMB. The residuals smaller than −1 s are plotted as squares; those ranging from −1 to 1 s are plotted as crosses; and those larger than 1 s are plotted as circles. The sizes of the symbols are proportional to the magnitudes of the travel-time residuals; (b) same as (a), except that the residuals are corrected using a shear-velocity model by Stephen Grand (personal communication) for the effects of the mantle heterogeneity 300 km above the CMB; (c) averaged shear-velocity perturbations in the bottom 300 km of the mantle inferred from the corrected travel-time residuals in (b). The shear-velocity perturbations are further averaged over 1° × 1° grids with a Gaussian cap with a radius of 1°; and (d) variation of thickness of the seismic anomaly inferred from the corrected travel-time residuals in (b) assuming a uniform average shear-velocity reduction of −5% for the anomaly. The lateral averaging procedure is the same as in (c). The black traces in (a–d) mark the geographic boundary determined from the corrected ScS–S travel-time residuals in (b).

and 4b). In the remainder of the text, we only present the results corrected based on the shear-velocity tomographic model by Grand. It is also interesting to note slightly negative correlations are still observed between the S travel-time residuals and the ScS–S travel residuals after the tomographic corrections (Fig. 4c and 4e). Such negative correlations likely indicate existence of some seismic anomalies in the mid-lower

mantle that are not accounted for by any of the tomographic models.

A transitional boundary from a region with negative or zero travel-time residuals (high or normal velocity) to a region with positive travel-time residuals (low velocity) is evident, and can be clearly mapped out (Fig. 3b). Smaller-scale variations of the ScS–S differential travel-time residuals are also present. For
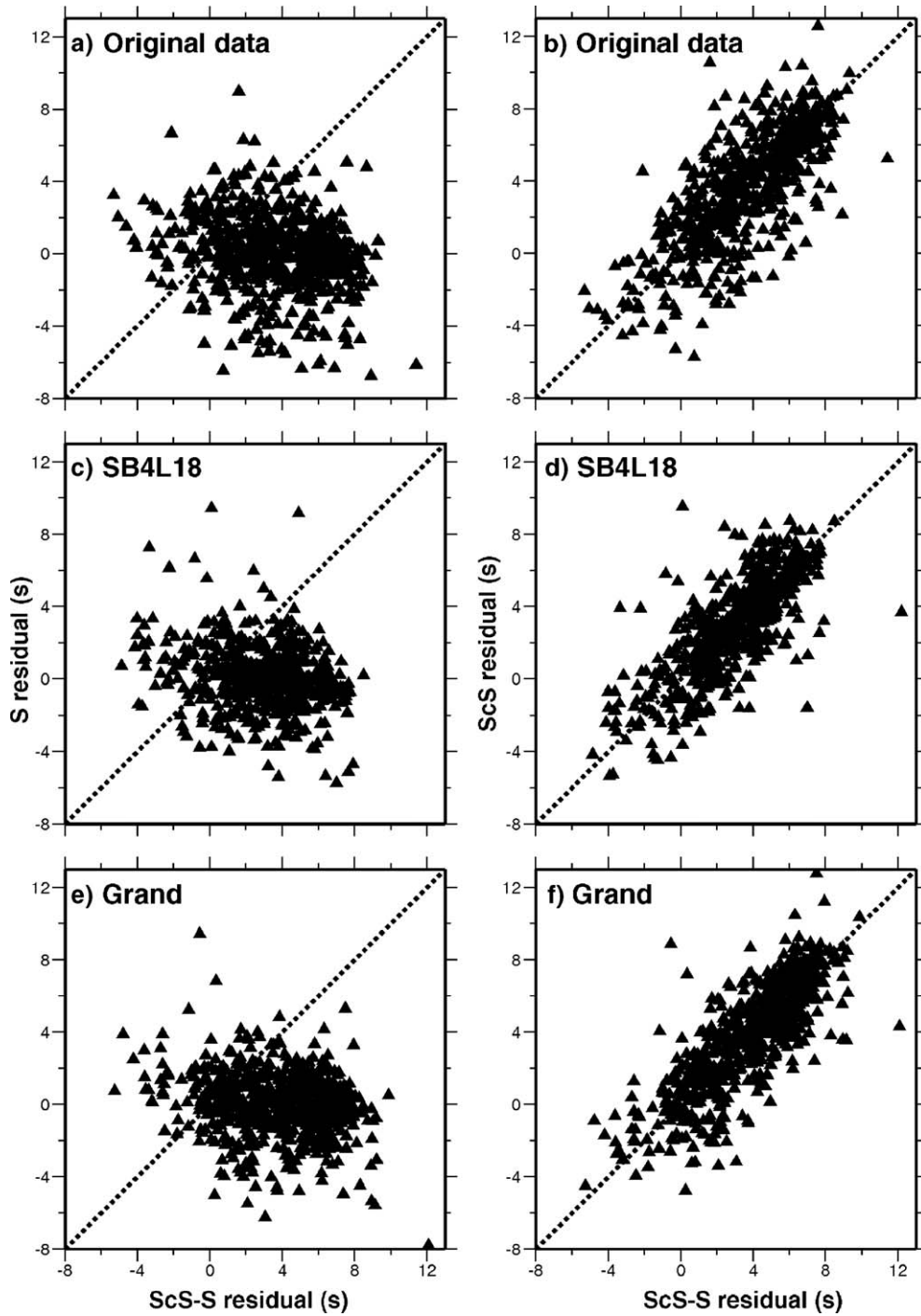
Fig. 4. (a, c, e) Relationship between observed S travel-time residuals and ScS–S differential travel-time residuals before (a) and after the corrections for the effects of the seismic heterogeneities 300 km above the CMB based on a shear wave tomographic model by Masters et al. [2] (c) and Grand (personal communication) (e). (b, d, f) same as (a, c, e), except for relationship between observed ScS travel-time residuals and ScS–S differential travel-time residuals. S and ScS times are hand-picked from the seismograms and corrected for array station statics. The dashed lines have a slope of 1 and intercept at (0, 0).

example, around (12°N, 155°E), a region with large positive travel-time residuals is surrounded by regions with small positive travel-time residuals. Such small-scale variations appear to be robust features, as the travel-time residuals obtained from several earthquakes recorded at different stations show a consistent pattern. The observed ScS–S differential travel-time residuals can be used to place constraints on the shear-velocity reductions in the lowermost 300 km of the mantle. Because the ScS–S differential travel-time residuals have limited resolution in constraining the vertical distribution of the seismic structures, as most of the ScS phases propagate sub-vertically in these distances, we only discuss vertically averaged velocities. We present two simple models to illustrate the lateral variation of the seismic structure and to place bounds on the magnitude of velocity reductions in the region. In the

first case, we assume that the ScS–S differential travel times are caused by a 300-km thick layer with lateral variations of shear-velocity. The inferred velocity perturbations show a lower-than-average velocity region surrounded by normal or high-velocity regions beneath the northwestern Pacific and Australia (Fig. 3c). To account for the magnitude of the ScS–S differential travel-time residuals, the average velocity perturbations in the lowermost 300 km of the mantle range from −5% to 4%. In general, the magnitude of the low velocity reduction increases from northwest to southeast and reaches about −5% around (5°S, 165°E) over a distance of about 800 km. In the second case, we assume that the ScS–S differential travel-time residuals are caused by a layer with a uniform average velocity reduction of −5% with laterally varying thickness. The thickness of the low-velocity anomaly varies from 300 to 0 km (Fig. 3d).
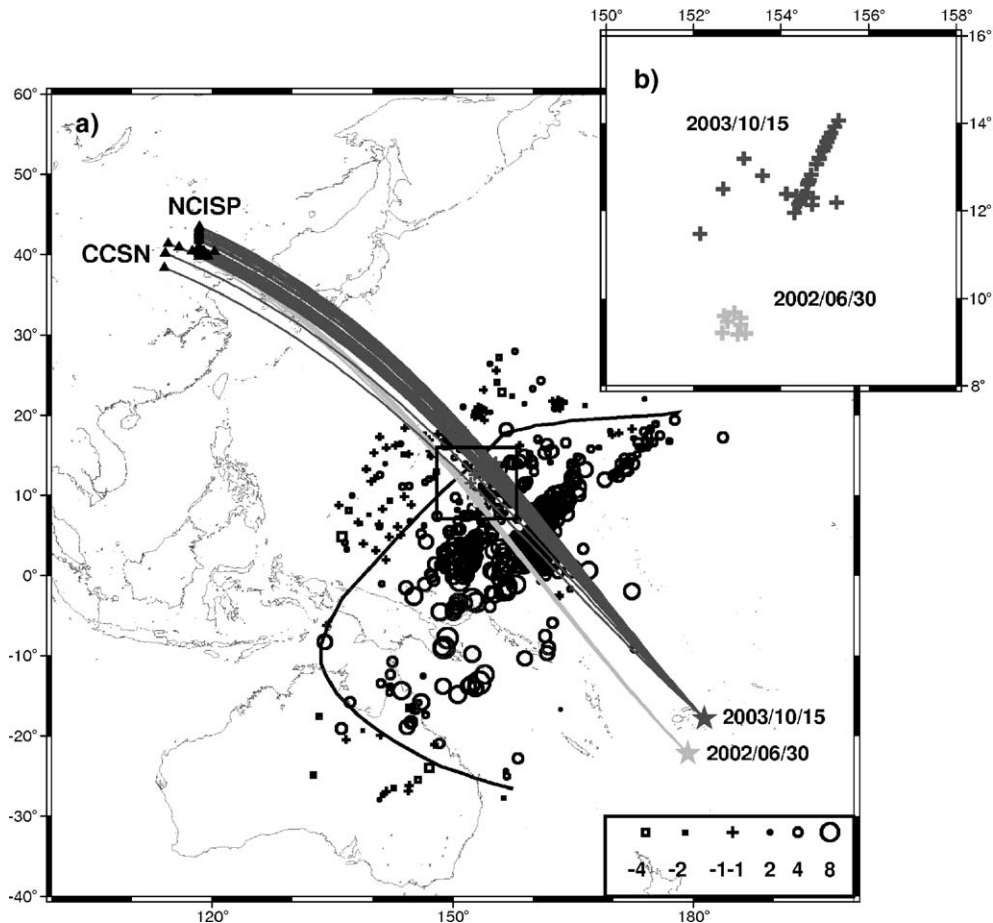

Fig. 5. (a) ScS reflected points (crosses) at the CMB, along with earthquakes (stars), seismic stations (triangles), and great-circle paths (gray lines), for the two events whose waveforms are used to constrain the detailed seismic structure in the edge of the anomaly. The corrected ScS–S differential time residuals in Fig. 3b are also plotted as background. The box indicates a region where detailed information of ScS reflected points is shown in (b). (b) ScS bounce points at the CMB shown as crosses for events 2003/10/15 and 2002/06/30.

3.2. Detailed seismic structure in the edge of the anomaly from waveform modeling

To constrain the nature of the transition from the low-velocity region to the high-velocity region, we select seismic waveform data recorded in the NCISP and the CCSN for two earthquakes, 2002/06/30 and 2003/10/15 occurring in the Tonga–Fiji subduction zone for waveform modeling. The ScS phases of these two events sample the anomaly across its northwestern boundary (Fig. 5), providing an ideal dataset for constraining the fine seismic structure in the edge of the anomaly.

The observed tangential displacements for event 2003/10/15 exhibit complex waveforms in close distances (Fig. 6a). The ScS phases are delayed compared to the predictions based on PREM (Fig. 6a). There exist two strong phases in the time window between S and ScS phases. One phase is evident immediately following the

direct S phase and has the same polarity as S (the phase labeled as Scd). The Scd phase is followed by a strong phase that has an opposite polarity to the SH and ScS phases (phase labeled as Sbc+SuS) (Fig. 6a). The amplitude of the Sbc+SuS phase is comparable to that of the S phase and has a move-out similar to the ScS phase. These complexities are not a result of a complicated earthquake source, as the recordings at other GSN stations show simple waveforms. Besides, the additional Scd and Sbc+SuS phases exhibit clear move-outs with epicentral distance.

The seismic data can be well explained by a model with a shear-velocity jump of 2% at 2746 km depth followed by a negative velocity gradient and a 30-km thick basal layer with a shear-velocity reduction of −13%. The discontinuity at 2746 km depth generates Scd+bc phases that fit the observed phases well. The onset depth of the discontinuity is well constrained by
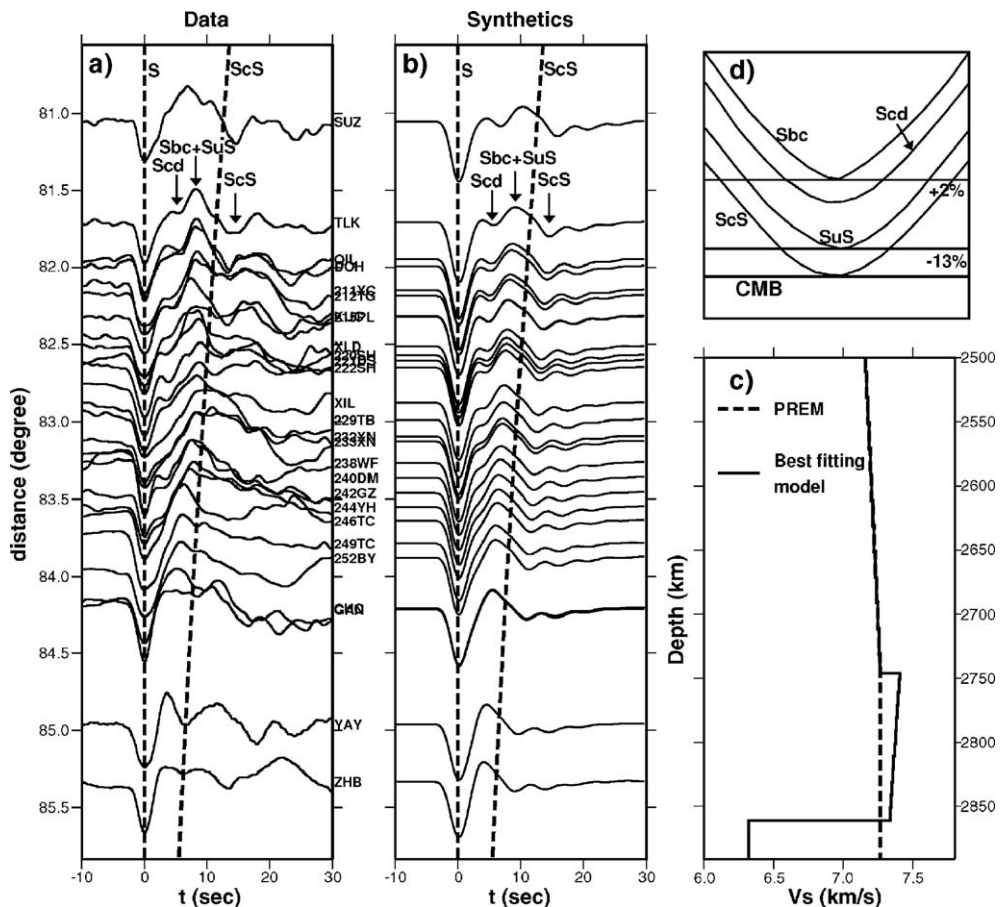

Fig. 6. (a) Tangential displacements recorded for event 2003/10/15. The seismic waveforms are aligned along the hand-picked SH maximum amplitudes; (b) synthetics calculated based on a one-dimensional (1D) model shown in (c). The dashed lines are predicted arrivals of S and ScS phases based on PREM; (c) 1D model (solid line) used for calculating synthetics in (b), along with PREM (dashed line); and (d) schematic illustration of the ray paths of Sbc, Scd, SuS and ScS phases generated by the 1D model. The arrivals of these phases are also labeled in the synthetics in (b).

the onset timing of the Scd phases. Synthetic tests indicate that the predicted Sbc phase alone is far too weak to account for the observed amplitudes of the phase labeled Sbc+SuS. An additional strong phase with an opposite polarity to the direct SH phase would be required to explain the observations. A 30-km thick basal layer with a large velocity reduction is invoked to explain the strong amplitudes of the Sbc+SuS phase. In this case, the SuS is the reflection off of the top of the basal layer. The sign of the observed SuS phase requires a decrease of velocity in the layer and the observed strong amplitude of the SuS phase requires a large velocity reduction inside the layer. Synthetic tests indicate that the amplitude of the Sbc+SuS phase is sensitive more to the shear-velocity reduction than to the density contrast of the basal layer. The relative timing between SuS and ScS phases further requires the thickness of the basal layer to be small when the velocity reduction of the layer is large. Overall, synthetics generated by our best-fitting model fit the observations well (Fig. 6b). The relative timing

between the SuS and S phases is also consistent with the inferred higher-than-average velocity between 2746 and 2861 km depths in the model. A shear-velocity reduction of −13% inside the basal layer produces synthetics that best fit the observations, but there are some trade-offs between thickness and velocity reduction of the basal layer. Models with the thickness varying from 40 to 23 km with corresponding velocity reduction changing from −9% to −17% would generate synthetics that fit the observations reasonably well. A minimum shear-velocity reduction of −9% is, however, required to explain the strong SuS phases and weak ScS phases observed in the data, and a shear-velocity reduction greater than −17% would generate too weak ScS phases to be consistent with the data. Synthetic tests indicate that the shear-velocity jump of the positive velocity discontinuity between 2746 and 2861 km trades off the onset depth of the discontinuity. A higher velocity jump with a larger onset depth of the discontinuity would explain the seismic data equally well. However, a minimal velocity
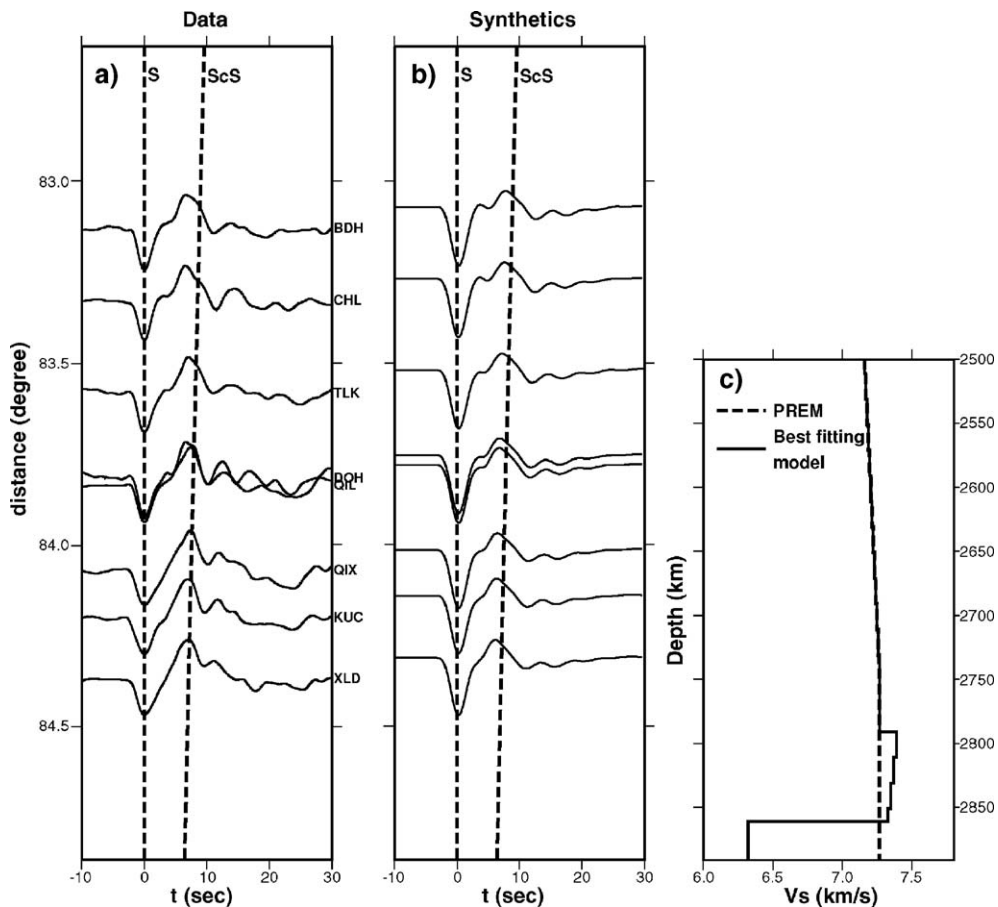

Fig. 7. (a) Observed tangential displacements for event 2002/06/30; (b) synthetics calculated based on the model in (c). The dashed lines are predicted arrivals of S and ScS phases based on PREM; and (c) 1D model (solid line) used to generate the synthetics, along with PREM (dashed line) as reference.
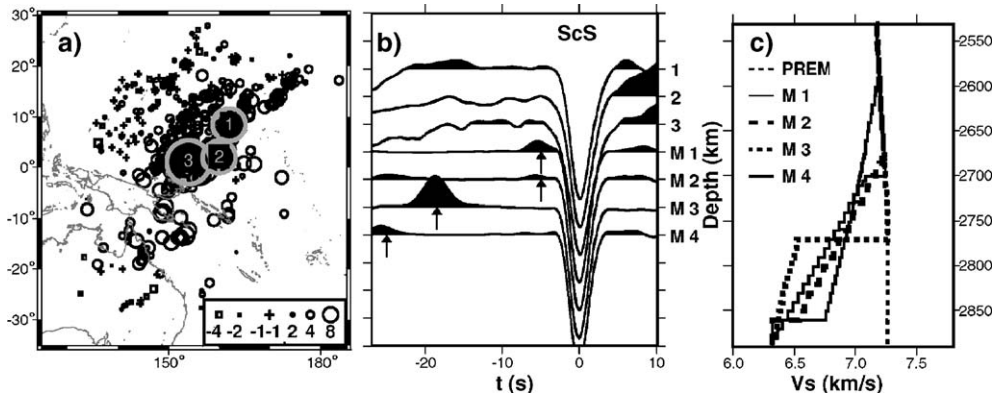
Fig. 8. (a) Three regions (gray circles) where the observed tangential displacements are stacked. The background shows the corrected ScS–S differential time residuals plotted at the ScS reflected points at the CMB; (b) stacked seismograms (top three traces) for three regions labeled accordingly as their ScS sampling regions in (a) and stacked synthetics for four models (bottom four traces). Black arrows show the reflected signals produced by velocity discontinuities in the models; (c) 1D models along with PREM (thin dashed line).

jump of 2% of the discontinuity is required to explain the seismic data and such trade-offs do not affect the inference of the velocity reduction of the basal layer.

The tangential displacements for event 2002/06/30 exhibit similar complexities and variations of waveforms (Fig. 7a) as those for event 2003/10/15. The Sbc +SuS pulse is more delayed than that of event 2003/10/15. This feature can be modeled by changing the onset depth of the positive discontinuity from 2746 to 2791 km with other parameters remaining the same. Overall, the seismic data can be well explained by a model with a shear-velocity increase of 2% relative to PREM at 100 km above the CMB and a 30-km thick basal layer with a shear wave velocity reduction of −13% (Fig. 7b and 7c).

3.3. Shear-velocity structure of the "Pacific anomaly"

We consider the low-velocity basal layer inferred from the above waveform modeling as a thin portion of the "Pacific anomaly" extending beneath the surround-
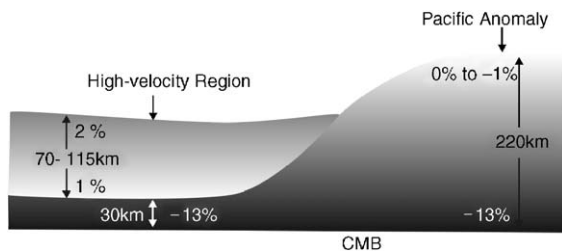

Fig. 9. Inferred seismic structure across the "Pacific anomaly". The anomaly has a strong negative velocity gradient from 0% to −1% to about −13% in the lowermost 220 km of the mantle and is surrounded by a high-velocity region with a positive discontinuity of 2% at about 100–145 km above the CMB. Portion of the "Pacific anomaly" spreads out beneath the surrounding high-velocity region.

ing high-velocity region. With the velocity reduction in the base constrained by the waveform data, we explore the best possible velocity structure that would satisfy both the inferred velocity reductions at the bottom of the anomaly and the ScS–S differential travel-time residuals in the middle of the anomaly. We stack the seismic data sampling three regions that have large ScS–S differential time residuals and dense sampling (Fig. 8a) to place bounds on possible velocity discontinuity structures in the middle of the anomaly. Only data with simple source-time functions are used in the stacking. There are at least 50 data in each stacking zone. All traces are self-normalized and summed along the hand-picked ScS phases. Synthetic stacks are performed following the same procedures as the data stacks. We fix the velocity reduction at the bottom of the mantle to be −13% and test models with the low-velocity structure extending to various depths, with the constraint that the predicted ScS–S differential travel-time residuals from all these models must fit the observations. Synthetic tests indicate that a velocity decrease of −2% or greater would generate a strong ScS precursor that would have been detected by the data stacks (Fig. 8b and 8c). The seismic data thus favor a strong negative velocity gradient from 0% to −1% at about 2671 km depth to −13% at the CMB in the middle of the anomaly, with the basal portion of the anomaly extending beneath the surrounding high-velocity region (Fig. 9).

4. Discussions

Using differential travel-time residuals of the long-period ScS–SH and sScS–sS phases, Wysession et al. [24,25] investigated the shear-velocity structure in the CMB region from 50°S to 50°N in latitude and 70°E to

190°E in longitude. Their inferred shear-velocity variations ranged from greater than 3% beneath Australia to −1.5% beneath northeastern Indonesia and Micronesia. Our inferred high-velocity structures in the region surrounding the "Pacific anomaly" is similar to the value they obtained (3%). Our inferred shear-velocity reductions inside the "Pacific anomaly" are much lower than the value (−1.5%) reported in their studies. The discrepancy is probably due to the different data coverage between the two studies and the waveforms used in our study in inferring the shear-velocity structures. Our low velocity reductions are inferred from the additional ScS–S differential travel times used in this study for the ScS phases sampling the middle of the "Pacific anomaly" and based on waveform modeling of the strong phases observed between ScS and S phases (Figs. 6, 7). Overall, two studies are not inconsistent with each other. Our inferred velocity perturbations are similar with those deduced from forward modeling of differential travel time in the lowermost mantle beneath the central Pacific [26].

The inferred velocity structure at the base of the mantle beneath the western Pacific is similar to those near the CMB beneath the south Atlantic and Indian Oceans [8]. Such a negative velocity gradient can be explained by partial melting of a compositional anomaly produced early in the Earth's history and a thermal gradient in the bottom thermal boundary layer [5,7]. In this partial melt scenario, an increase of temperature in the bottom thermal boundary layer would generate an increasing fraction of melt with depth. An increasing fraction of melt and an increase of temperature result in a strong negative shear-velocity gradient in the lowermost several hundred kilometers of mantle [5–7]. Wen et al. [5] also suggested that a compositional anomaly produced early in the Earth's history would have these two characteristics: it may be enriched in less compatible elements (e.g., Fe, Al) and even some volatile elements, and these elements may significantly depress its solidus; and it may be enriched in heat-producing elements, such as U, Th and K, and internal temperatures may be so elevated inside the anomaly. Both these two characteristics would explain why such a compositional anomaly would be preferentially partially molten.

The inferred velocity structure in the edge of the anomaly can be explained by a scenario that the basal portion of the "Pacific anomaly" spreads out beneath the surrounding high-velocity region (Fig. 9). The seismic structure above the 30 km basal layer in the surrounding region is typical of the D″ velocity structure in most of the high-velocity regions [27–37]. A phase change from perovskite to post-perovskite may explain the positive discontinuities at 100–145 km above the CMB [38,39].

A strong negative velocity gradient at the base of the "Pacific anomaly" would suggest that the observed positive ScS–S travel-time residuals can be more reasonably explained by a model of varying thickness at the base of the anomaly (for example, the model in Fig. 3d). In this case, although the horizontal sampling region of the ScS phases in the bottom 220 km is large, the geographic boundary delineated based on the corrected ScS–S travel-time residuals (Fig. 3) likely accurately marks the geographic extent of the "Pacific anomaly" because of the dense coverage of the seismic data and the presumed small thickness of the anomaly near the boundary based on the ScS–S differential travel-time residuals there.

The observed small-scale variations of seismic structure within the "Pacific anomaly" appear to be consistent with the seismic evidence for the existence of ultra-low velocity zones near the CMB beneath western Pacific [40–42,20]. This characteristic of the "Pacific anomaly" is different from that of the "African anomaly", which appears to be relatively uniform inside.

5. Conclusions

We determine geographical boundary and the shear-velocity structure of the base of the "Pacific anomaly" beneath the western Pacific Ocean based on waveform modeling and travel-time analysis of ScSH–SH phases. The northwestern geographic boundary is determined on the basis of the observed ScS–SH differential travel-time residuals. The magnitude of the ScS–S differential travel-time residuals suggests that the average shear-velocity reduction inside the "Pacific anomaly" reaches −5% in the lowermost 300 km of the mantle. Waveform modeling suggests that the northwestern boundary is characterized by a shear-velocity model with a velocity jump of about 2% at about 100–145 km above the CMB and a 30-km thick basal layer with a shear wave velocity reduction of −13%, while the stacked seismic data exclude any internal discontinuity with a velocity decrease greater than −2% in the middle of the anomaly. Overall, the seismic data sampling the base of the "Pacific anomaly" can be explained by a negative shear-velocity gradient from 0% to −1% (top) to −13% (bottom) in the lowermost 220 km of the mantle, similar to those of a very-low velocity province beneath the South Atlantic Ocean and the Indian Ocean. Such a strong negative shear-velocity gradient can be explained by partial melting of a compositional anomaly produced early in the Earth's history situated in a bottom thermal

boundary layer. The seismic structures found in the edge of the anomaly can be explained by a scenario that the partially molten portion of the "Pacific anomaly" spreads out beneath the surrounding high-velocity regions, and the positive discontinuity at about 100–145 km above the CMB may be explained by a phase change from perovskite to post-perovskite. Our travel time data also indicate the existence of internal small-scale seismic heterogeneities inside the "Pacific anomaly".

Acknowledgments

References

[1] Y.J. Gu, A.M. Dziewonski, Mantle discontinuities and 3-D tomographic models, EOS Trans. AGU 80 (1999) F717.

[2] G. Masters, G. Laske, H. Bolton, A. Dziewonski, The relative behavior of shear velocity, bulk sound speed, and compressional velocity in the mantle: implications for chemical and thermal structure, in: S. Karato, A.M. Forte, R.C. Liebermann, G. Masters, L. Stixrude (Eds.), Earth's Deep Interior, AGU Monograph, vol. 117, AGU, Washington D.C., 2000, pp. 63–87.

[3] C. Mégnin, B. Romanowicz, The three-dimensional shear velocity structure of the mantle from the inversion of body, surface and higher-mode waveforms, Geophys. J. Int. 143 (2000) 709–728.

[4] J. Ritsema, H.-J. van Heijst, Seismic imaging of structural heterogeneity in Earth's mantle: evidence for large-scale mantle flow, Sci. Prog. 83 (2000) 243–259.

[5] L. Wen, P. Silver, D. James, R. Kuehnel, Seismic evidence for a thermo-chemical boundary at the base of the Earth's mantle, Earth Planet. Sci. Lett. 189 (2001) 141–153.

[6] L. Wen, Seismic evidence for a rapidly varying compositional anomaly at the base of the Earth's mantle beneath the Indian Ocean, Earth Planet. Sci. Lett. 194 (2001) 83–95.

[7] L. Wen, An SH hybrid method and shear velocity structures in the lowermost mantle beneath the central Pacific and South Atlantic Oceans, J. Geophys. Res. 107 (2002), doi:10.1029/2001JB000499.

[8] Y. Wang, L. Wen, Mapping the geometry and geographic distribution of a very low velocity province at the base of the Earth's mantle, J. Geophys. Res. 109 (2004), doi:10.1029/2003JB002674.

[9] Y. Wang, L. Wen. Geometry and P- and S-velocity structures of the "African anomaly". J. Geophys. Res. (submitted for publication).

[10] S. Ni, D.V. Helmberger, Seismological constraints on the South African superplume; could be the oldest distinct structure on earth, Earth Planet. Sci. Lett. 206 (2003) 119–131.

[11] A.M. Dziewonski, D.L. Anderson, Preliminary reference earth model, Phys. Earth Planet. Inter. 25 (1981) 297–356.

[12] E.J. Garnero, S.P. Grand, D.V. Helmberger, Low P-wave velocity at the base of the mantle, Geophys. Res. Lett. 20 (1993) 1843–1846.

[13] E.J. Garnero, D.V. Helmberger, Further structure constraints and uncertainties of a thin laterally varying ultralow-velocity layer at the base of the mantle, J. Geophys. Res. 103 (1998) 12495–12509.

[14] Q. Williams, J. Revenaugh, E. Garnero, A correlation between ultra-low basal velocities in the mantle and hot spots, Science 281 (1998) 546–549.

[15] T. Lay, Q. Williams, E.J. Garnero, The core–mantle boundary layer and deep earth dynamics, Nature 392 (1998) 461–468.

[16] L. Wen, D.V. Helmberger, Ultra-low velocity zones near the core-mantle boundary from broadband PKP precursors, Science 279 (1998) 1701–1703.

[17] J. Mori, D.V. Helmberger, Localized boundary layer below the mid-pacific velocity anomaly identified from a PcP precursor, J. Geophys. Res. 100 (1995) 20359–20365.

[18] J.E. Vidale, M.A.H. Hedlin, Evidence for partial melt at the core–mantle boundary north of Tonga from the strong scattering of seismic waves, Nature 391 (1998) 682–685.

[19] L. Wen, D.V. Helmberger, A two-dimensional P-SV hybrid method and its application to modeling localized structures near the core–mantle boundary, J. Geophys. Res. 103 (1998) 17901–17918.

[20] M.S. Thorne, E.J. Garnero, Inference on ultralow-velocity zone structure from a global analysis of SPdKS waves, J. Geophys. Res. 109 (2004), doi:10.1029/2004JB 003010.

[21] J. Ritsema, E.J. Garnero, T. Lay, A strongly negative shear velocity gradient and lateral variability in the lowermost mantle beneath the Pacific, J. Geophys. Res. 102 (1997) 20395–20411.

[22] M.E. Wysession, A. Langenhorst, M.J. Fouch, K.M. Fischer, G.I. Al-Eqabi, P.J. Shore, T.J. Clarke, Lateral variations in compressional/shear velocities at the base of the mantle, Science 284 (1999) 120–125.

[23] A. To, B. Romanowicz, Y. Capdeville, N. Takeuchi, 3D effects of sharp boundaries at the borders of the African and Pacific Superplumes: observation and modeling, Earth Planet. Sci. Lett. 233 (2005) 137–153.

[24] M.E. Wysession, L. Bartkó, J.B. Wilson, Mapping the lowermost mantle using core-reflected shear waves, J. Geophys. Res. 99 (1994) 13,667–13,684.

[25] M.E. Wysession, L. Bartkó, J.B. Wilson, Correction to "Mapping the lowermost mantle using core-reflected shear waves", J. Geophys. Res. 100 (1995) 8351.

[26] L. Bréger, B. Romanowicz, Three-dimensional structure at the base of the mantle beneath the central Pacific, Science 282 (1998) 718–720.

[27] T. Lay, D.V. Helmberger, A lower mantle S-wave triplication and the shear velocity structure of D″, Geophys. J. R. Astron. Soc. 75 (1983) 799–838.

[28] C.J. Young, T. Lay, Evidence for a shear velocity discontinuity in the lower mantle beneath India and the Indian Ocean, Phys. Earth Planet. Inter. 49 (1987) 37–53.

[29] J.B. Gaherty, T. Lay, Investigation of laterally heterogeneous shear velocity structure in D″ beneath Eurasia, J. Geophys. Res. 97 (1992) 417–435.

[30] E.J. Garnero, D.V. Helmberger, S. Grand, Preliminary evidence for a lower mantle shear wave velocity discontinuity beneath the central Pacific, Phys. Earth Planet. Inter. 79 (1993) 335–347.

[31] J.M. Kendall, P.M. Shearer, Lateral variations in D″ thickness from long-period shear wave data, J. Geophys. Res. 99 (1994) 11575–11590.

[32] J.M. Kendall, P.M. Shearer, On the structure of the lowermost mantle beneath the southwest Pacific, southeast Asia and Australasia, Phys. Earth Planet. Inter. 92 (1995) 85–98.

[33] T. Lay, E.J. Garnero, C.J. Young, J.B. Gaherty, Scale lengths of shear velocity heterogeneity at the base of the mantle from S wave differential travel times, J. Geophys. Res. 102 (1997) 9887–9909.

[34] S. Bilek, T. Lay, Lower mantle heterogeneity beneath Eurasia imaged by parametric migration of shear waves, Phys. Earth Planet. Inter. 108 (1998) 201–218.

[35] C. Thomas, T. Heesom, J.M. Kendall, Investigating the heterogeneity of the D″ region beneath the northern Pacific using a seismic array, J. Geophys. Res. 107 (2002), doi:10.1029/2000JB000021.

[36] E.J. Garenero, T. Lay, D″ shear velocity heterogeneity, anisotropy and discontinuity structure beneath the Caribbean and central America, Phys. Earth Planet. Inter. 140 (2003) 219–242.

[37] T. Lay, E.T. Garnero, S.A. Russell, Lateral variation of the D″ discontinuity beneath the Cocos Plate, Geophys. Res. Lett. 31 (2004), doi:10.1029/2004GL020300.

[38] A.R. Oganov, S. Ono, Theoretical and experimental evidence for a post-perovskite phase of $MgSiO_3$ in Earth's D″ layer, Nature 430 (2004) 445–448.

[39] M. Murakami, K. Hirose, K. Kawamura, N. Sata, Y. Ohishi, Post-perovskite phase transition in $MgSiO_3$, Science 304 (2004) 855–858.

[40] E.J. Garnero, D.V. Helmberger, A very slow basal layer underlying large-scale low-velocity anomalies in the lower mantle beneath the Pacific: evidence from core phases, Phys. Earth Planet. Inter. 91 (1995) 161–176.

[41] E.J. Garnero, D.V. Helmberger, Seismic detection of a thin laterally varying boundary layer at the base of the mantle beneath the central-Pacific, Geophys. Res. Lett. 23 (1996) 977–980.

[42] E.J. Garnero, J. Revenaugh, Q. Williams, T. Lay, L.H. Kellogg, Ultralow velocity zone at the core–mantle boundary. The core–mantle boundary region, Geodynamics, vol. 28, the American Geophysical Union, 1998, pp. 319–334.